

RESEARCH ARTICLE

# GBStools: A Statistical Method for Estimating Allelic Dropout in Reduced Representation Sequencing Data

Thomas F. Cooke<sup>1</sup>, Muh-Ching Yee<sup>2</sup>, Marina Muzzio<sup>1,3,4</sup>, Alexandra Sockell<sup>1</sup>, Ryan Bell<sup>1</sup>, Omar E. Cornejo<sup>1,5</sup>, Joanna L. Kelley<sup>1,5</sup>, Graciela Bailliet<sup>6</sup>, Claudio M. Bravi<sup>4,6</sup>, Carlos D. Bustamante<sup>1</sup>, Eimear E. Kenny<sup>1,3,7,8,9\*</sup>

**1** Department of Genetics, Stanford University, Stanford, California, United States of America, **2** Carnegie Institution for Science, Department of Plant Biology, Stanford, California, United States of America, **3** Charles Bronfman Institute of Personalized Medicine, Icahn School of Medicine at Mount Sinai, New York, New York, United States of America, **4** Facultad de Ciencias Naturales y Museo, Universidad Nacional de La Plata, La Plata, Argentina, **5** School of Biological Sciences, Washington State University, Pullman, Washington, United States of America, **6** Instituto Multidisciplinario de Biología Celular (CCT La Plata-CONICET, CICIPBA), La Plata, Argentina, **7** Department of Genetics and Genome Sciences, Icahn School of Medicine at Mount Sinai, New York, New York, United States of America, **8** Institute of Genomics and Multiscale Biology, Icahn School of Medicine at Mount Sinai, New York, New York, United States of America, **9** Center of Statistical Genetics, Icahn School of Medicine at Mount Sinai, New York, New York, United States of America

\* [eimear.kenny@mssm.edu](mailto:eimear.kenny@mssm.edu)



 OPEN ACCESS

**Citation:** Cooke TF, Yee M-C, Muzzio M, Sockell A, Bell R, Cornejo OE, et al. (2016) GBStools: A Statistical Method for Estimating Allelic Dropout in Reduced Representation Sequencing Data. *PLoS Genet* 12(2): e1005631. doi:10.1371/journal.pgen.1005631

**Editor:** William A. Cresko, University of Oregon, UNITED STATES

**Received:** March 27, 2015

**Accepted:** October 7, 2015

**Published:** February 1, 2016

**Copyright:** © 2016 Cooke et al. This is an open access article distributed under the terms of the [Creative Commons Attribution License](https://creativecommons.org/licenses/by/4.0/), which permits unrestricted use, distribution, and reproduction in any medium, provided the original author and source are credited.

**Data Availability Statement:** All sequencing data have been deposited in the Short Read Archive (SRA) under accessions PRJNA300277 and PRJNA303086. Exome array data have been deposited at the European Genome-phenome Archive (EGA) under accession EGAS00001001663.

**Funding:** GB and CMB received funding from Consejo Nacional de Investigación Científica y Tecnológica (CONICET; <http://www.conicet.gov.ar/?lan=en>) and the Agencia Nacional de Promoción Científica y Tecnológica (<http://www.agencia.mincyt.gob.ar/>), Argentina. MM received funding from the

## Abstract

Reduced representation sequencing methods such as genotyping-by-sequencing (GBS) enable low-cost measurement of genetic variation without the need for a reference genome assembly. These methods are widely used in genetic mapping and population genetics studies, especially with non-model organisms. Variant calling error rates, however, are higher in GBS than in standard sequencing, in particular due to restriction site polymorphisms, and few computational tools exist that specifically model and correct these errors. We developed a statistical method to remove errors caused by restriction site polymorphisms, implemented in the software package GBStools. We evaluated it in several simulated data sets, varying in number of samples, mean coverage and population mutation rate, and in two empirical human data sets (N = 8 and N = 63 samples). In our simulations, GBStools improved genotype accuracy more than commonly used filters such as Hardy-Weinberg equilibrium p-values. GBStools is most effective at removing genotype errors in data sets over 100 samples when coverage is 40X or higher, and the improvement is most pronounced in species with high genomic diversity. We also demonstrate the utility of GBS and GBStools for human population genetic inference in Argentine populations and reveal widely varying individual ancestry proportions and an excess of singletons, consistent with recent population growth.

Pew Charitable Trusts (<http://www.pewtrusts.org/en>). The funders had no role in study design, data collection and analysis, decision to publish, or preparation of the manuscript.

**Competing Interests:** The authors have declared that no competing interests exist.

### Author Summary

Eukaryotic genomes range from millions to billions of base pairs in size, but for many genetic experiments it is sufficient to gather information from just a fraction of these sites. In practice, selecting a consistent set of sites can be achieved by cutting genomic DNA with enzymes that recognize DNA sequence motifs, and then sequencing the ends of the resulting fragments. The advantages of this well-known approach are its low cost relative to whole-genome sequencing (WGS) and that it does not require a sequenced genome. These methods, for example genotyping-by-sequencing (GBS), are popular for mapping genes and studying population genetics, particularly in non-model organisms. Here we demonstrate, however, that computational tools designed for WGS are insufficient for handling certain error types that arise in GBS and other similar methods. We present a modified protocol for GBS and a statistical method for detecting these errors, implemented in the software package GBStools. We tested our methods on human DNA samples from Argentine populations. Our results reveal widely varying degrees of European and Native American ancestry, and that rare genetic variants are more numerous than would be expected in a population with constant size.

### Introduction

High-throughput reduced-representation sequencing methods[1] are inexpensive, suffer little from ascertainment bias, and generate genetic markers that are approximately randomly distributed throughout the genome. These methods have been successfully used in trait mapping [2,3], linkage map construction[1,4], selection scans[5,6], and estimating genetic diversity[7]. One such method is genotyping-by-sequencing[8] (GBS). In GBS, the sequencing target is reduced to < 5% of the genome by ligating sequencing adapters only to restriction enzyme cut sites (Fig 1A). GBS reads can also be assembled into short contigs, which enables single nucleotide variant (SNV) calling without the aid of a genome sequence[9]. Hence, GBS is a popular approach in non-model systems, which typically lack resources such as genome assemblies and microarrays.

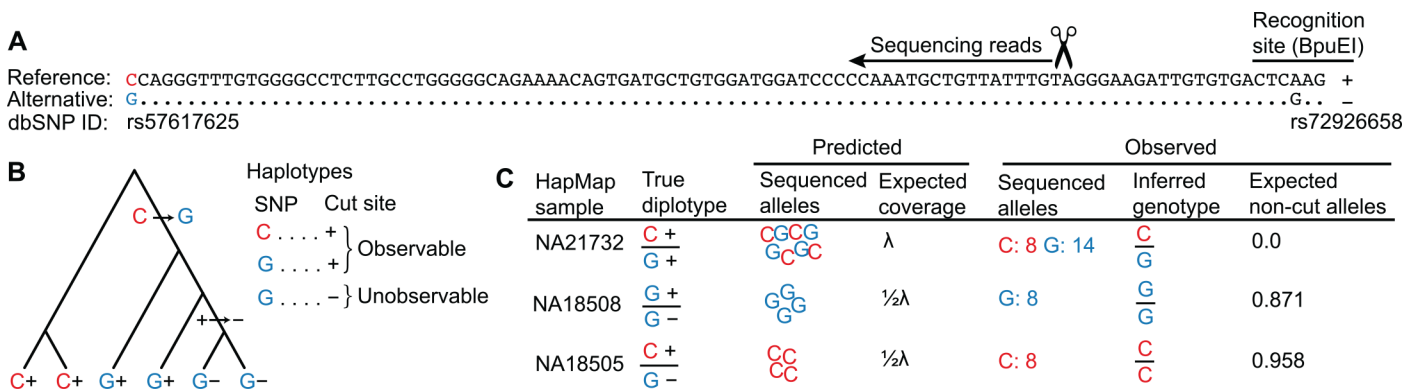


**Fig 1. Incorrect inference of genotypes due to restriction site polymorphism.** **A.** GBS reads spanning the SNP rs57617625 originated from a polymorphic BpuEI site 94 bp upstream. The non-cut BpuEI allele caused by SNP rs72926658 is labeled as '-' and the cut allele '+'. **B.** The '-' allele arose on the haplotype with the derived G allele, causing some G alleles to be unobservable by GBS. **C.** The samples shown carried the three possible heterozygous diplotypes. The sequencing results were consistent with the predictions. Sample NA18505 was incorrectly called homozygous, but the expected non-cut allele count calculated by GBStools (0.958) closely matched the true count (1), identifying it as a probable mis-call.

doi:10.1371/journal.pgen.1005631.g001

Unlike whole genome sequencing (WGS), GBS is prone to variant calling errors due to restriction site polymorphisms [7,10–14] ('allelic dropout', Fig 1B). Allelic dropout in GBS can confound applications that rely on accurate calling of rare variation, such as site frequency spectrum estimation in population genetics. Here, we present a modified GBS protocol, similar to ddRAD-seq [15], and quantify its error rate. In addition, we present a systematic statistical approach to detect allelic dropout in GBS sequence data, implemented in the open-source software package GBStools.

This approach is based on the fact that allelic dropout reduces a sample's read coverage at a particular site in proportion to the number of non-cut restriction site alleles it carries there (Fig 1C). Therefore GBStools models coverage of each sample at a particular site as an overdispersed Poisson random variable drawn from either a distribution with mean  $\lambda$  (zero non-cut alleles carried), a distribution with mean  $\frac{1}{2}\lambda$  (one non-cut allele), or with mean zero (two non-cut alleles). GBStools calculates the maximum-likelihood estimate of the parameter  $\lambda$  by expectation-maximization (EM), with the true number of non-cut alleles per sample serving as latent (unobserved) variables (S1 Appendix). The expected values of these latent variables can be used to estimate which samples carry a non-cut allele (see "Expected non-cut alleles" in Fig 1C). Simultaneously, GBStools estimates the site frequency of the observable reference and alternative SNP alleles,  $\phi_1$  and  $\phi_2$  (for example see Fig 1B), and the non-cut allele,  $\phi_3$ , where  $\phi_1 + \phi_2 + \phi_3 = 1$ . Finally, it performs a likelihood ratio test comparing the null hypothesis  $\phi_3 = 0$  to the alternative hypothesis  $\phi_3 > 0$ . In its current implementation GBStools cannot infer the true genotypes obscured by allelic dropout, but it can be used to remove errors by filtering out sites where a high likelihood ratio indicates the presence of restriction site polymorphism.

Lastly, we describe the application of these methods to an extant mixed ancestry population from Argentina to test the performance of GBS in ancestry estimation and demographic inference.

## Results and Discussion

We estimated the magnitude of GBS errors caused by restriction site polymorphisms from both simulated and real data. We chose human as a model system for GBS methods development due to the availability of a high-quality reference genome assembly, high-coverage whole-genome sequencing data, [16,17] and dense SNP array data.

First, we prepared modified GBS libraries from eight HapMap samples from a diverse range of populations and sequenced them on a single HiSeq lane (S1 Table, methods). We used the methylation-insensitive enzymes BpuEI, BsaXI, and CspCI, which cut away from their recognition site. Although a well-balanced mix of different sequencing adapters is commonly used to ensure that restriction enzyme recognition sequences are not over-represented at the start of the sequencing reads [3,4,8,15], our method tolerates low-diversity mixes of adapters, which is convenient when working with smaller sample sets. We quantified each sample by bioanalyzer after PCR, but before pooling, with the goal of reducing variance in the number of reads per sample in the final library. We found, however, that errors at this stage, particularly those caused by incorrect quantification of the bioanalyzer internal standard, can in fact lead to the opposite effect (S1 Fig). More careful quantification by bioanalyzer, or quantification by fluorimetry, should correct this problem and lead to the desired effect. The HapMap samples had 16.7X mean coverage in a 128 Mb target region (S2A and S3A Figs). We used GATK [18] to call SNPs in the target regions, and found 483,381 segregating sites that passed variant quality score recalibration. After applying hard filters (coverage  $\geq 8X$  in 8/8 samples, mapping quality  $\geq 57$ , SNP quality  $\geq 30$ ), these GBS genotype calls were 98.0% concordant with heterozygous calls from whole-genome sequencing data gathered from the same set of samples

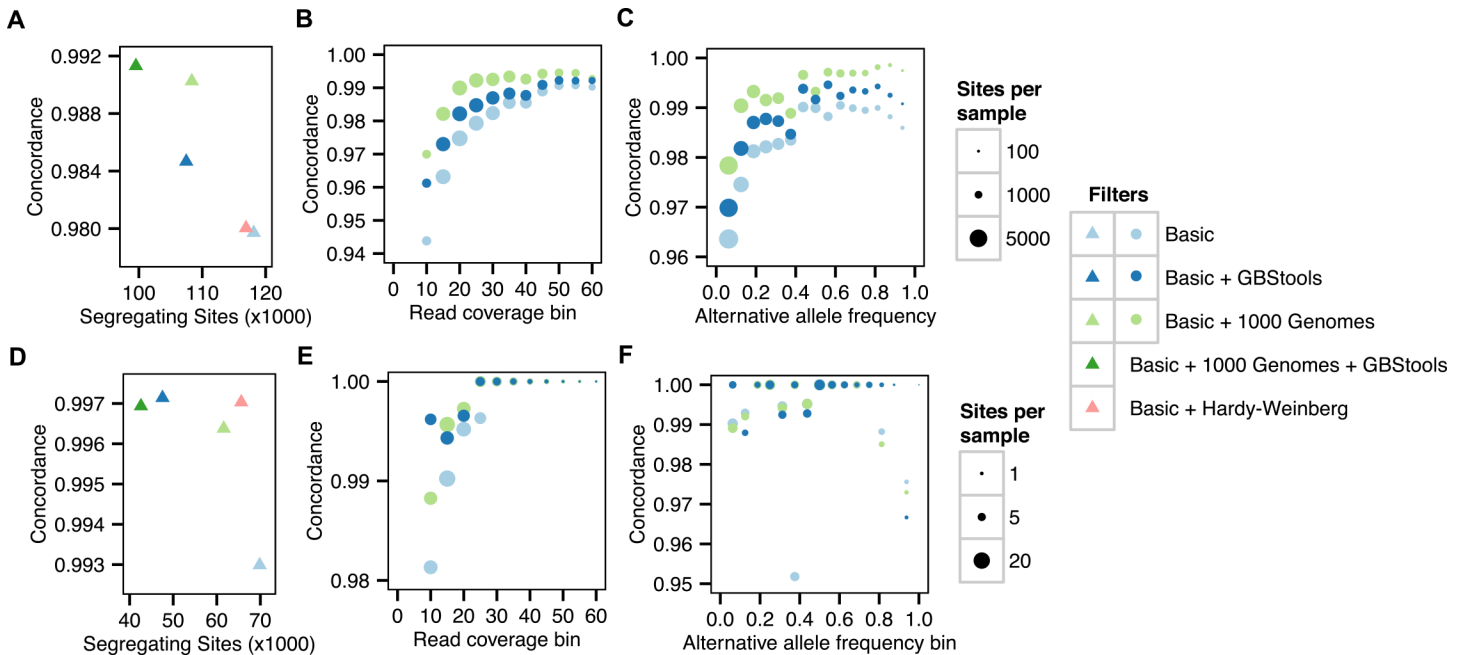


**Fig 2. Concordance before and after applying GBS SNP filters.** **A.** Proportion of GBS genotype calls concordant with Complete Genomics heterozygote calls for HapMap individuals vs number of segregating sites after applying various filters. Sites passing the basic filters had: mapping quality  $\geq 57$ , SNP quality  $\geq 30$ , coverage  $\geq 8X$  in all samples, and position outside the 1000 Genomes Project callability mask. Sites failing the GBStools filter had: Non-cut allele frequency estimate  $> 0.05$ , or likelihood ratio  $> 2.71$  ( $p < 0.05$ ). Sites failing the 1000 Genomes filter had  $> 10\%$  of spanning reads mapped to known polymorphic restriction site (allele frequency  $> 0.01$ ). **B.** Same data as in A, but with genotypes binned by depth of coverage. **C.** Same data as A-B, but with genotypes binned by alternative allele frequencies, which were inferred from whole genome sequencing of the eight HapMap individuals (two sequenced by SOLiD technology, and six sequenced by Complete Genomics). **D-F.** Same analysis as A-C, but for concordance between GBS genotypes calls and exome array calls for the Argentine individuals. Basic filters are same as in A-C, but require  $\geq 8X$  coverage in  $\geq 40/63$  samples. Allele frequencies were estimated from genotypes of 389 Argentine individuals on the exome array.

doi:10.1371/journal.pgen.1005631.g002

(Fig 2A and S2A Table). We found the error rate dropped as sequencing coverage increased up to 30-40X, after which further increases in coverage had little effect (Fig 2B). Furthermore, the error rate for singletons was roughly two-fold higher than for non-singletons (Fig 2C). A filter for known restriction site polymorphisms in the 1000 Genomes Project [19] data set also had a strong effect on concordance (Fig 2A-2C). These three factors appeared to be the major determinants of genotype calling accuracy.

The fact that hard filters resulted in a fairly low error rate (2%) suggested that this is a sensible approach for species with genetic diversity similar to humans. But many non-model organisms have higher levels of genetic diversity, which may lead to an error rate that is high enough to necessitate a more sophisticated approach. To explore this possibility, we simulated GBS data under a neutral coalescent model [20] with population mutation rates ( $\theta = 4N\mu$ ) between  $1 \times 10^{-3}$ – $2 \times 10^{-2}$ . In a preliminary filtering step, we removed SNVs with  $> 10\%$  missing genotypes, which reduced the genotype error rate to 1.2% for data simulated with  $\theta = 1 \times 10^{-3}$  (typical of human data), and 4.7% for data simulated with  $\theta = 5 \times 10^{-3}$ , which is typical of high-diversity species such as *Drosophila* (S4A Fig). We simulated 40X GBS coverage for these same genotype data, and found that the GBStools likelihood ratio test reduced the error more than 10-fold, for instance down to 0.3% in the case of the high-diversity ( $\theta = 5 \times 10^{-3}$ ) data set (S4A Fig). Although normalized site frequency spectra (SFS) were not substantially affected by restriction site polymorphisms (S4D and S4E Fig), errors in the genotypes themselves may cause problems in some applications. In these cases, particularly in studies of high diversity species, GBStools is expected to improve genotyping accuracy more than hard filters.

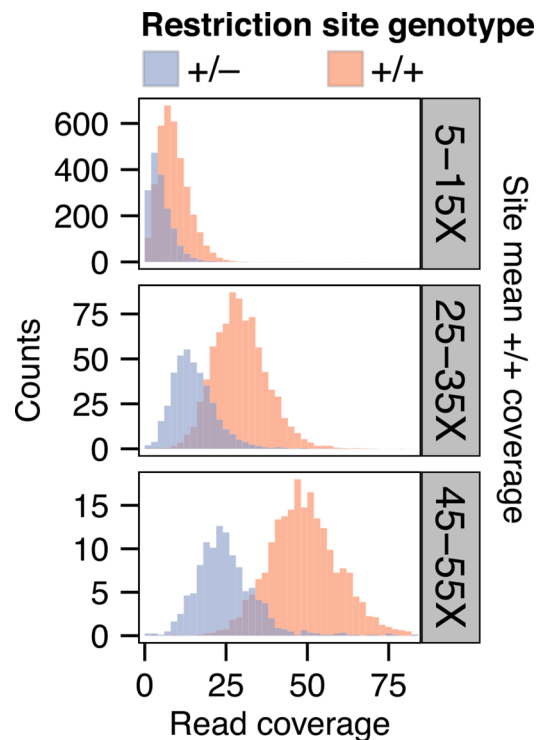


**Fig 3. Read coverage distributions at sites with a known restriction site polymorphism.** Distributions of normalized depth of GBS coverage for HapMap individuals with one non-cut restriction site allele (genotype +/-) or with two intact restriction site copies (genotype +/+) at sites with a known restriction site polymorphism.

doi:10.1371/journal.pgen.1005631.g003

As a preliminary step in testing the utility of GBStools, it was necessary to confirm the theoretical prediction that samples with one non-cut restriction site allele (restriction site genotype +/-) have on average half the coverage of samples with two intact restriction site alleles (restriction site genotype +/+). To test this, we measured GBS coverage at known polymorphic restriction sites in the HapMap data (Fig 3). We applied a normalization to account for variation in total read numbers between libraries (methods), and binned the individual sample coverages according to the mean coverage of +/+ samples at each site. Within each bin, we observed two distinct, but overlapping, coverage distributions for samples with restriction site genotypes +/- and +/+, suggesting that the prediction holds true. The proportion of the +/- distribution that does not overlap the +/+ distribution provides a rough measure of the potential power of a statistical test for restriction site polymorphism based on read coverage, and it is evident from the extensive overlap of the two distributions in the 5-15X and 25-35X bins that higher coverage is necessary to achieve substantial power. If the goal of a particular study were to estimate population-level summary statistics such as  $F_{st}$ , or to map traits in an experimental cross, the added accuracy afforded by such a test might not be worth the extra sequencing effort to achieve > 35X coverage. If the goal, however, were to estimate the site frequency spectrum, then high genotype accuracy would be necessary, and in such cases (e.g. exome sequencing) coverage in the > 35X range is not uncommon. Thus the conditions for high-sensitivity detection of restriction site polymorphisms might already exist in many experimental designs.

To better define the experimental conditions under which it is possible to use GBStools effectively, we applied GBStools to data simulated with different numbers of samples (from  $N = 8$  to  $N = 500$ ), and read coverages (10-100X). Since the proportion of homozygotes at a



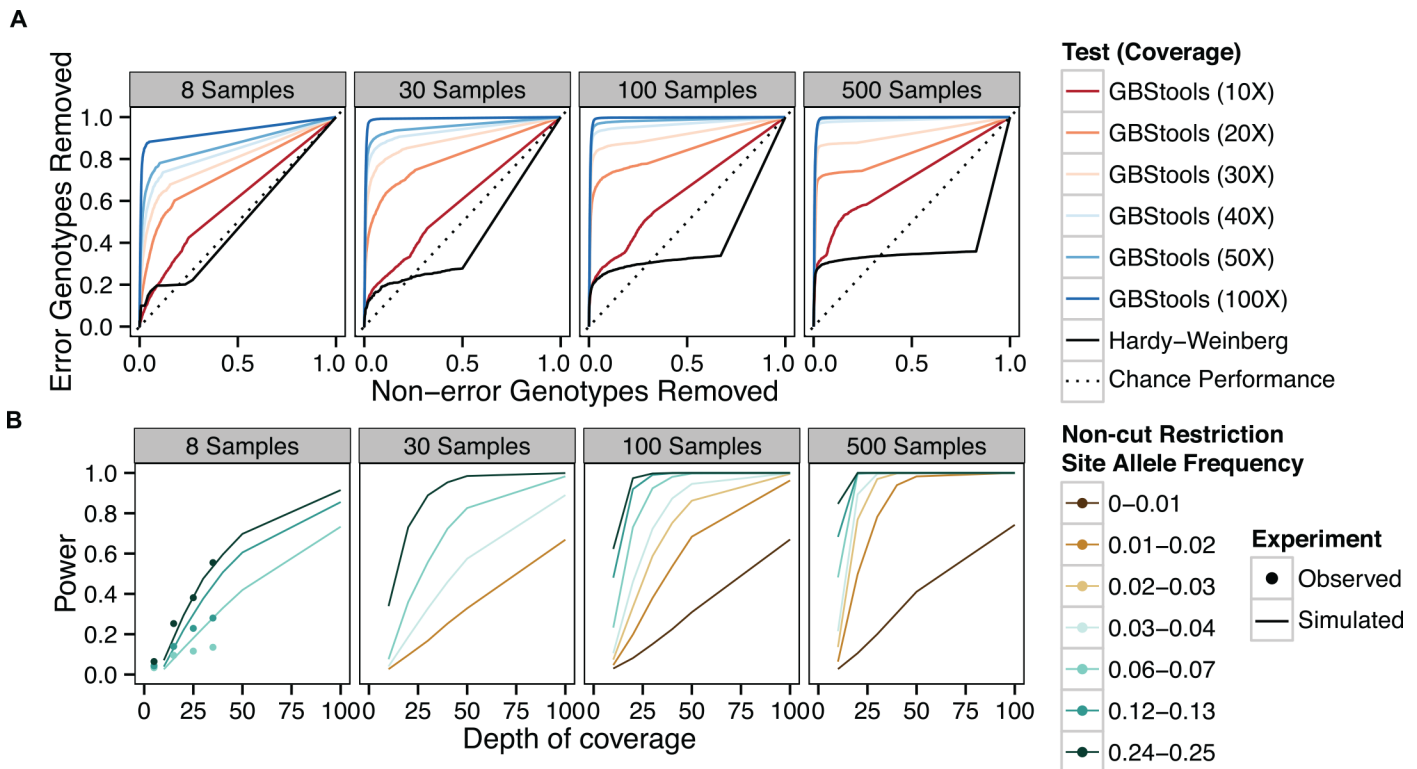


**Fig 4. Sensitivity and specificity of GBStools likelihood ratio test vs sample number.** **A.** Response operator characteristic (ROC) curves for classification of incorrect vs correct heterozygote genotype calls by GBStools likelihood ratio test or Hardy-Weinberg equilibrium exact test p-values. The data were filtered by call rate (sites with > 10% missing genotypes were excluded) before applying either test, and the axes refer to the proportion of genotypes that passed this filter. The diagonal represents performance of an uninformative (random) classifier. **B.** Power of GBStools likelihood ratio test for detecting restriction site polymorphism with simulated and empirical data. We used a critical value of 2.71 for calculating power, based on the expected null distribution, a one-half chi-squared distribution with one degree of freedom ( $p < 0.05$ ). Empirical power was calculated for 331,861 autosomal SNPs in the HapMap GBS data set that passed insert size filters and where the EM parameter estimates converged (see [Methods](#)).

doi:10.1371/journal.pgen.1005631.g004

SNV observed by GBS is sometimes inflated by restriction site polymorphism, we also used an exact test to assess the chance of observing the given genotypes (or a worse-fitting set of genotypes) at each site under Hardy-Weinberg equilibrium. We then calculated the sensitivity and specificity of the GBStools likelihood ratio, or the Hardy-Weinberg p-values, as classifiers of incorrect vs correct genotype calls under varying thresholds ([Fig 4A](#)), and measured the area under curve (AUC) of the response operator characteristic (ROC) curves as indicators of the test's performance. In theory, an uninformative (random) classifier has  $AUC = 0.5$ , whereas a perfect classifier has  $AUC = 1.0$ . The GBStools test outperformed the Hardy-Weinberg test as measured by area under the curve (AUC), particularly at high-coverage sites ([Fig 4A](#), [S3 Table](#)). We noted that the ROC curves for the GBStools test at low coverage (10X) and the Hardy-Weinberg test have a similar shape, which may be due to the assumption of Hardy-Weinberg genotype proportions in the GBStools model ([S1 Appendix](#)). Aside from the already-established benefit of high coverage, we also found that large sample sizes were beneficial to GBStools performance. For example, power to detect non-cut restriction site alleles of frequencies between 0.01–0.02 was 25% for 30 samples at 40X coverage, but was 94% for 500 samples at the same coverage ([Fig 4B](#)). For 40X sites in the 100- and 500-sample data sets, AUC was at least 0.96, suggesting that this is the ideal coverage and sample size range for using GBStools.

At lower coverage (10-20X) and with smaller sample sets ( $N = 8$ ) GBStools did not perform as well in simulations (Fig 4), and this may explain the modest increase in concordance from 98.0% to 98.5% when the GBStools filter was applied to the HapMap data set ( $N = 8$ ), which led to the removal of 9% of segregating sites (Fig 2A). For comparison, a filter for known restriction site polymorphisms in the 1000 Genomes Project [19] data set improved concordance to 99.0% (Fig 2A, S2C Table), suggesting that the power of GBStools was no higher than 50%. Indeed, power to detect common restriction site polymorphisms in the HapMap GBS data (non-cut allele frequency 0.25) was 56% for sites covered to 30-40X, but for singleton sites covered to 30-40X it was only 13%, which was lower than predicted by simulation (Fig 4B). In addition, AUC values for the HapMap ROC curves were lower than the values obtained in simulations with matching coverage levels (Fig 5A, S3 Table). This is possibly due to the model's assumption of a constant value for the index of dispersion in depth of coverage between samples, whereas the empirical data exhibit variation in dispersion from site to site (S5 Fig). It should be possible to relax this assumption by estimating dispersion on a site-by-site basis, or by calculating a joint estimate from genome-wide data, but these methods are currently not implemented. Joint modeling of genotypes at multiple closely-linked SNPs should also offer an increase in power over the single-marker model currently implemented. This would be particularly useful in the case of long reads, where each "stack" of reads mapped to a particular restriction site would contain more SNPs on average than a stack of shorter reads. For the present time, however, our simulations suggest the easiest way to improve the low empirical power observed here is to increase the number of samples.

We investigated whether it is possible to accurately estimate which particular genotypes are likely to be affected by allelic dropout. As mentioned in the introduction, the true numbers of non-cut alleles per sample are latent variables in the GBStools likelihood model, and the expected values of these variables are output by GBStools in VCF format. We compared these expected non-cut allele counts to the true counts inferred from whole-genome sequencing data to gain an idea of their predictive value (Fig 6). Although samples with a true allele count of one (i.e. restriction site genotype +/-) had higher average expected non-cut allele counts than samples with true allele count of zero (genotype +/+), it is clear that this is not a very sensitive predictor. For instance, +/- samples at sites with non-cut allele frequency 0.25 and 30-40X coverage had a median expected non-cut allele count of 0.01 (Fig 6), far from the true value of 1.0. Yet power to detect restriction site variants in these same data was 56% (Fig 4B). This indicates that the true utility of GBStools is in determining whether or not any samples at a site carry non-cut alleles rather than determining which particular samples carry them, although in some cases (Fig 1C) there is diagnostic value in the latter approach.

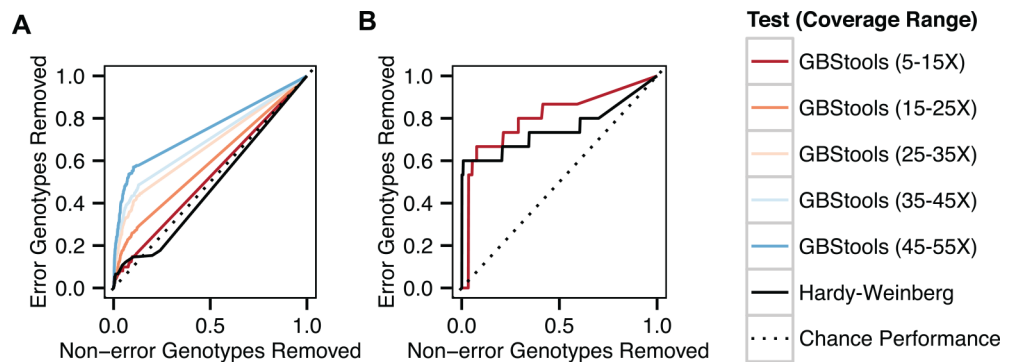


**Fig 5. Empirical sensitivity and specificity of GBStools test.** **A.** Response operator characteristic (ROC) curves, as in Fig 4A, for GBStools and Hardy-Weinberg tests with HapMap data. The data were filtered by coverage, call rate, and mapping quality (methods), before applying either test. **B.** Same as (A), but for Argentine data set.

doi:10.1371/journal.pgen.1005631.g005

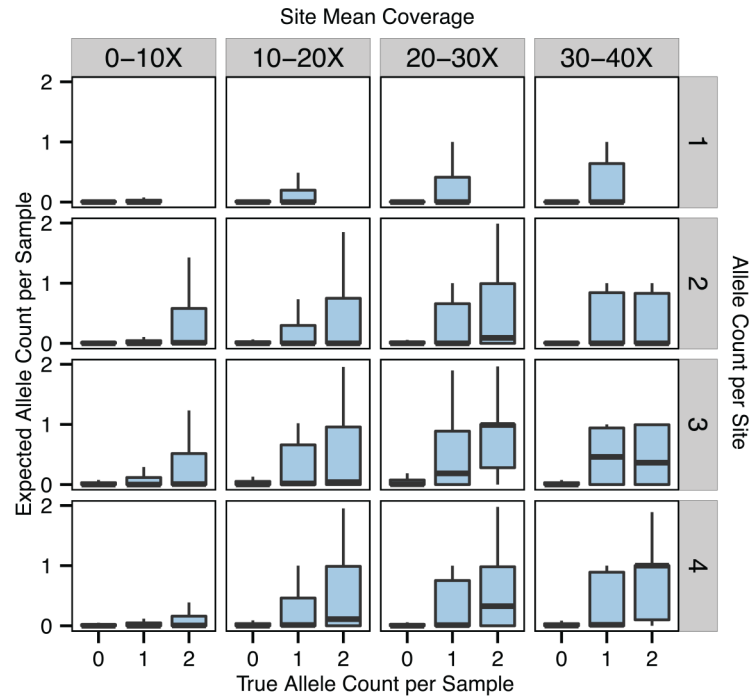


**Fig 6. Expected non-cut restriction site allele counts.** The true numbers of non-cut restriction site alleles carried by each sample are latent variables in the GBStools likelihood model. Boxplots representing the distributions of the expected values of these variables are shown here, and are grouped by the true non-cut allele counts inferred from Complete Genomics whole-genome sequencing data for HapMap samples. Allele counts of 0, 1 and 2 correspond to restriction site genotypes +/+, +/- and -/- respectively, where (-) is the non-cut allele. Plots are also grouped by site allele count (with 8 samples total) and site mean coverage. Only sites with allele frequencies between 0.0625–0.25 are shown.

doi:10.1371/journal.pgen.1005631.g006

The site frequency spectrum derived from our filtered GBS data was similar to the spectrum from whole-genome sequencing data, with 2.3% fewer singletons (Fig 7A). This suggested that GBS data can be useful in population genetic studies, for example demographic inference based on the site frequency spectrum.

To explore this further, we sequenced 89 admixed Argentine individuals to test for signatures of mixed ancestry and demographic changes (S4 Table). The Argentine samples had 7.5X mean coverage in a 177 Mb target region (S3B Fig, S4 Table). Argentine samples with < 30% of reads mapped to restriction sites (26/89 samples) were excluded from further analyses, as it is likely that these samples were not digested to completion. A total of 1,013,785 segregating sites were called in the remaining samples and concordance with exome array data was 99.7% after filtering with GBStools, which led to removal of 25% of sites (Fig 2D, S3H and S3K Table). A filter for Hardy-Weinberg equilibrium showed similar sensitivity and specificity (Fig 5B), although fewer segregating sites were removed (Fig 2D), indicating the GBStools critical value we used was more conservative. Both tests performed better than expected in simulations with a similar number of samples (N = 100). This is probably due to the small number of errors that remained after applying basic filters (15 in total, see S3 Table), and the fact that over half of these errors originated from a single SNP (rs6861689) that is near a common restriction site polymorphism (BsaXI site overlapping rs6861731).

We calculated the expected SFS from the Argentine GBS data and compared it to the SFS under a neutral coalescent model, and to the SFS from 386 Argentine individuals genotyped on



an exome SNP array (Fig 7B). The excess of singletons in the GBS spectrum is consistent with recent population growth,[21] but was not observed in the array data, most likely due to ascertainment bias. Another potential area where GBS can be useful is in ancestry estimation. We joined the Argentine GBS data set with SNP data from Yoruban, European, and Mexican individuals from the 1000 Genomes Project[19] phase 1 data set, and from Maya individuals from the Human Genome Diversity Project, and performed principal components analysis (Fig 7C, methods). As expected, individuals from the admixed Argentine populations fell between the European and Native American populations in PC space.

In summary, we have used high-quality human SNP chip and whole-genome sequencing resources to test several different methods for reducing genotype errors in GBS data, including commonly-used hard filters, and a new GBS-specific statistical method implemented in our open-source program GBStools. These methodological improvements enable GBS to nearly match whole-genome sequencing in accuracy, as we have demonstrated, but at a fraction of the cost. Furthermore, our simulations suggested that GBStools has substantially better performance than hard filters in high diversity species with extensive restriction site polymorphism. Since GBStools is designed to accept data in the standard VCF format (and can optionally use read data in the standard SAM/BAM format), it can supplement many pre-existing GBS variant calling pipelines, for example the one implemented in the program Stacks[22]. We anticipate that this approach may enable many GBS-based analyses beyond high-throughput trait mapping, in particular population genetics studies such as detecting signatures of hitchhiking and selection, and estimating demographic history.

## Methods

### Data availability statement

All sequencing data have been deposited in the Short Read Archive (SRA) under accessions PRJNA300277 and PRJNA303086. Exome array data have been deposited at the European Genome-phenome Archive (EGA) under accession EGAS00001001663.

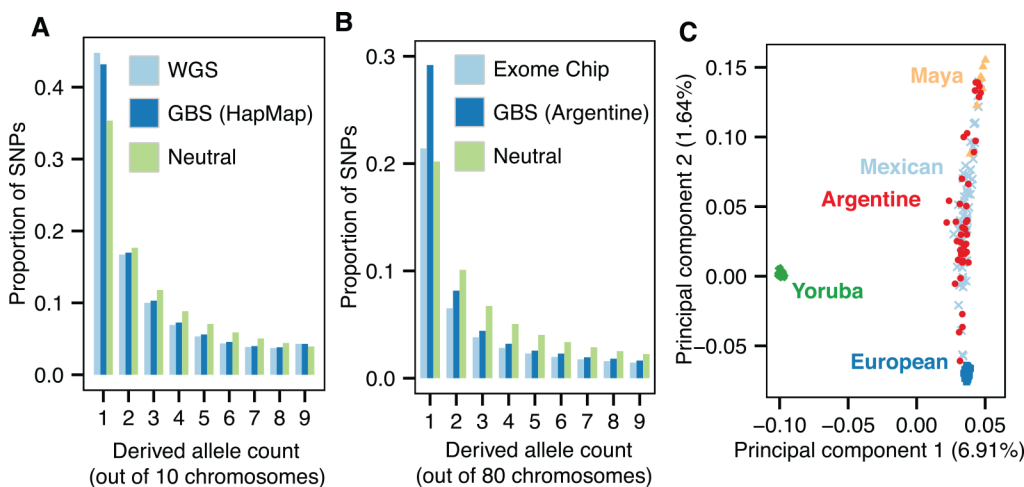


**Fig 7. Detecting population structure and growth with GBS data.** **A.** Normalized site frequency spectra (SFS) of the derived allele for six HapMap samples represented as the expected SFS of a subsample of size five to account for missing data. SNPs from the 29.2 Mb region that passed all filters were used for both GBS and whole-genome sequencing (WGS) spectra. The expected SFS under a neutral coalescent model is shown for comparison. **B.** Bins 1–9 of the normalized SFS for SNPs in the Argentine GBS data set, represented as the expected SFS of a subsample of size 40. Exome chip data was from 386 Argentine individuals, including some of those sequenced by GBS. **C.** Principal components 1 and 2 of the admixed Argentine individuals, Europeans (CEU), Yoruba (YRI), Mexican (MXL), and Maya (HGDP), using 30,691 SNPs. Of the Argentine samples, 40/63 passed the 5% data missingness filter and were used in the PCA.

doi:10.1371/journal.pgen.1005631.g007

## Ethics statement

Genomic DNA from eight HapMap individuals, including six samples sequenced by Complete Genomics[16] and two samples sequenced with SOLiD technology[17], was obtained from Coriell Cell Repositories. The Argentine samples were collected from 15 geographical regions in Argentina in multiple sampling efforts between 2007–2012. Under local IRB approval, blood samples were collected from participants who gave informed consent. Both HapMap and Argentine samples were de-identified and analyzed anonymously.

## Simulation of GBS data

We used Hudson's *ms*[20] to generate  $1 \times 10^7$  random samples of 200 haplotypes at a 500 bp-long locus with a population mutation rate of  $1 \times 10^{-3}$  ( $\theta = 4N_e\mu$ ) without recombination. The position of each segregating site within the locus was drawn from a uniform distribution. The first and last 6 bp of the locus represented two 6 bp-long restriction enzyme recognition sites. If any segregating site fell within these two sites, a restriction site polymorphism resulted, and either the derived or ancestral allele was randomly chosen to represent the non-cut restriction site allele. Segregating sites in the interior of the fragment, but farther than 6 bp from the ends, were chosen to represent restriction site polymorphisms with probability 0.0074 (the frequency of bases that are part of BpuEI, BsaXI, and CspCI recognition sites in the human genome). Segregating sites within 101 bp of the fragment ends represented sites sequenced by GBS with paired-end 101 bp reads. We randomly paired the 2N haplotypes to create a set of N diploypes. Heterozygous genotypes within the 'read' portion of diploypes that were heterozygous for one of the restriction sites were counted as genotyping errors. Simulations with population mutation rates of  $5 \times 10^{-3}$ ,  $1 \times 10^{-2}$ , and  $2 \times 10^{-2}$  were also carried out. As most loci simulated in this manner do not carry restriction site polymorphisms it is an inefficient way to simulate large numbers of them. Thus to simulate GBS data for estimating the power of the GBStools likelihood ratio test we randomly chose one segregating site per locus to represent a restriction site polymorphism, irrespective of its location, and randomly chose either the derived or ancestral allele to be the non-cut allele. Depth of coverage was drawn from a negative binomial distribution with mean  $\mu$  and scale parameter  $\mu / 1.5$  (dispersion index = 2.5). Read likelihoods were then calculated[18], assuming a constant sequencing error rate of  $1 \times 10^{-3}$ .

## Exome array genotype calls

Data for Illumina Human Exome Beadchip v1.0 (HumanExome-12v1\_A) were generated for the Argentine samples at the Hussman Institute for Human Genomics, University of Miami. Genotypes were called with Illumina's Genome Studio V2011.1 with a no-call threshold of 0.15. A minimum call rate of 99.3% was required for each sample and 386 of the 391 Argentinian samples passed this filter. Per-SNP quality filters included: mapping to a unique genomic location, and minimum per-SNP call rate of 99% (245,937 SNPs met these criteria). Of these sites, 8 were excluded from the concordance analysis for the reason that more than one sample had an exome array call of homozygous reference and a GBS call of homozygous non-reference (or vice versa).

## Whole genome sequencing variant calls

Variation data files (masterVar) for samples NA18505, NA18508, NA19648, NA19704, NA21732, and NA21733 were downloaded from the Complete Genomics ftp site. We generated a vcf file with the mkvcf utility (v1.6.0 build 43). Before calculating concordance with GBS calls, we removed low confidence and hemizygous genotype calls, and excluded 10 sites that

exhibited discordance with the GBS calls across the majority of samples. We used the unfiltered variant calls for site frequency spectrum estimation, but split multi-nucleotide polymorphisms into their component SNPs with a custom python script. We used another custom python script to predict BpuEI, BsaXI, and CspCI restriction site variants caused by bi-allelic SNPs and indels in the unfiltered calls. The sequencing of samples NA19740 and NA19836 was described previously[17]. We predicted restriction site polymorphisms caused by SNPs in these samples in the same manner.

## Library preparation

Genomic DNA (50 ng) was digested with BpuEI (2.5 U), BsaXI (2 U), and CspCI (2.5 U) (NEB) at 37° for 90–120 min in buffer containing 20  $\mu$ M S-adenosylmethionine. The digestion product was purified on a DNA Clean and Concentrate column (Zymo Research). DNA end repair, 3' monoadenylation, and ligation of sequencing adapters were performed as described in the Illumina TruSeq DNA Sample Preparation Guide. We designed a custom set of sequencing adapters, derived from the TruSeq adapters, with 65 six-bp barcodes (S5 Table). We used a standard protocol to anneal the common adapter to each of the 65 barcode adapters[8]. The ligation product was amplified by 10 cycles of PCR. For the HapMap samples, inserts between 350–650 bp were size selected on a Caliper Labchip, with one sample per gel lane. For the Argentine samples, inserts between 350–650 bp were size-selected in batches of 9–11 samples per gel lane. Bioanalyzer quantification was used to pool in equimolar amounts before and after size selection. For the 89 Argentine samples, two pools were prepared and sequenced separately, the first with 24 samples and the second with 65. Because of the high variance in read numbers per sample we observed in the Argentine libraries, we later re-analyzed the bioanalyzer data from the first set of 24 samples (S1 Fig).

## Sequencing and read mapping

Libraries were sequenced on the Illumina HiSeq 2000 in 2 x 101 bp mode following the standard TruSeq SBS protocol. The eight HapMap samples were sequenced on a single lane, with a mean of 18.3 M paired end reads per sample. In the Argentine study, the two pooled libraries were sequenced on four and five separate lanes respectively, with a mean of 17.5 M reads per sample. Reads were mapped to the human reference genome (build 37) with BWA[23] with the -q 20 parameter to include soft clipping of low quality bases. Local realignment of reads around known indels and base quality recalibration were performed with GATK[18]. We defined the target region for the HapMap samples by taking the union of predicted restriction site fragments between 400–700 bp that had  $\geq 3X$  mean coverage, and where  $\geq 10\%$  of reads had a mate pair mapped to a restriction site (S2A Fig). The target region for the Argentine samples was defined in the same way, but with predicted fragments between 200–600 bp. Argentine samples with  $< 30\%$  of reads mapped to restriction sites (26/89 samples) were excluded from further analyses.

## Calculation of coverage distributions at polymorphic restriction sites

For each of the HapMap samples in our GBS data set we inferred the number of cut and non-cut alleles at each restriction site in the genome from the Complete Genomics and SOLiD data. We then calculated depth of coverage and median insert size at each site. For this analysis we kept only sites where the median insert sizes were between 350–625 bp for each sample, and where  $\leq 4$  samples had zero depth of coverage. We normalized the depth of coverage for each

sample by multiplying by the following normalization factor:

$$norm_{ij} = \frac{\frac{1}{n} \sum_{k=1}^n r_{kj}}{r_{ij}} \quad (1)$$

Here  $n$  is the total number of samples, and  $r_{ij}$  is the total number of library inserts of size  $j$  for individual  $i$ . In calculating  $norm_{ij}$  for a particular site we took  $j$  to be the median insert size of reads from individual  $i$  at that site. We then binned each site according to the mean coverage of samples that had two restriction site copies. Then, aggregating the coverage data across samples, we plotted the coverage distributions for each bin.

## Variant calls and hard filters

We called SNPs in the target regions described above with the GATK Unified Genotyper, emitting both variant and invariant sites. We also used the GATK Haplotype Caller to call SNPs in the HapMap data set. We found that specificity was higher for Haplotype Caller, with fewer true homozygous reference genotype called heterozygous (S2F Table), but also found that sensitivity was lower, with fewer true SNPs called. It is possible that this was because we used Haplotype Caller parameters that are optimal for whole-genome sequencing but not for GBS. We did not explore this point further, however, and instead used the SNP calls from Unified Genotyper for the remainder of the analyses. We performed variant quality score recalibration on segregating sites with GATK with the following training data sets (downloaded from the Broad Insitute ftp server): hapmap\_3.3.b37.sites.vcf 1000G\_omni2.5.b37.sites.vcf. For the HapMap samples we also trained with known variants from previous whole-genome sequencing studies [16,17]. We trained VQSR with the annotations HaplotypeScore, QD, ReadPosRankSum and HRun, and kept sites in the 99% sensitivity tranche. Invariant sites were not subjected to the VQSR filter. We applied the following hard filters (labeled as 'basic filters' in figures and tables): mapping quality  $\geq 57$ , SNP quality  $\geq 30$ , coverage  $\geq 8X$  in all samples (HapMap samples) or coverage  $\geq 8X$  in  $\geq 40/63$  of samples (Argentine samples). We also filtered out sites that fell within the 1000 Genomes Project callability masks for depth of coverage and mapping quality. In addition, we applied a filter for sites where the observed genotypes differ significantly from those predicted under Hardy-Weinberg equilibrium ( $p < 0.05$ ), with the software package vcftools[24].

## 1000 Genomes Project polymorphic restriction site filter

We used a custom python script to predict BpuEI, BsaXI, and CspCI restriction site variants caused by SNPs and indels in the 1000 Genomes Project data set. For each sample we created a set of genomic intervals where more than five read pairs spanned a restriction site that was polymorphic with a minor allele frequency of  $> 0.01$ . We then filtered out all sites that fell within the interval set of more than one sample.

## GBStools polymorphic restriction site filter

The calculation of frequency estimates for non-cut restriction site alleles, and the calculation of the likelihood ratio test statistic for restriction site polymorphism are described in S1 Appendix. We implemented these algorithms in the python package GBStools (<http://med.stanford.edu/bustamantelab/software.html>). Frequency estimates for a non-cut restriction site allele are expected to be zero under the null hypothesis (no polymorphism). Since this is on the boundary of the parameter space (0, 1], the parameter estimate is expected to have a half-normal

distribution. Therefore, the test statistic is expected to have an approximately one-half chi-squared distribution with one degree of freedom[25], which has a critical value of 2.71 ( $p = 0.05$ ). We applied the likelihood ratio test to simulated GBS data and found that at high coverage the test statistic was equal to zero more often than expected (S6 Fig). In the 20–50X coverage range, however, it agreed well with the expected distribution. The departure from the expected null distribution at high coverage was related to the fact that more than half of the allele frequency estimates were zero (S7 Fig) and suggested that in general 2.71 is a lenient critical value ( $p < 0.05$ ) for detecting restriction site polymorphisms. We performed the likelihood ratio test for SNPs where the median insert size was between 450–625 bp (HapMap individuals) or 300–500 bp (Argentine individuals) and where the median absolute deviation in insert size was less than 60 bp (S8 Fig). For the 'GBStools filter' listed in the figures and tables, we kept only SNPs that had a likelihood ratio  $< 2.71$  and an estimated frequency of the non-cut restriction site allele  $< 0.05$ . In addition, we excluded the region spanned by the two restriction sites nearest to any site that did not meet these criteria.

### GBStools power calculation

We applied the likelihood ratio test described above to GBS data from the HapMap samples. We restricted the power analysis to autosomal sites that were segregating in the Complete Genomics data set, where the median GBS insert size was between 450–625 bp, and the median absolute deviation for insert sizes was  $\leq 60$  bp (331,861 sites). We binned the sites according to mean depth of coverage, and for each bin we calculated the power to detect known polymorphic restriction sites at a conservative critical value of 2.71 (empirical  $p = 0.05$  critical values were slightly lower).

### Site frequency spectra

We calculated the expected site frequency spectrum from GBS data and Complete Genomics data for HapMap samples NA18505, NA18508, NA19648, NA19704, NA21732, and NA21733 as a subsample of size five in order to allow for missing data[26,27]. We used 1000 Genomes inferred ancestral alleles, and discarded sites where the ancestral allele was not consistent with the observed alleles. We kept sites that passed variant quality score recalibration and passed the hard filters ('basic filters'), the 1000 Genomes Project restriction site polymorphism filter, and the GBStools filter (29.2 Mb of total unmasked sites). The whole-genome sequencing (Complete Genomics) site frequency spectrum was calculated based on segregating sites in this same region. We calculated the expected site frequency spectrum for the Argentine samples as a subsample of size 40 after applying the filters shown in S2 Fig (12.7 Mb of total unmasked sites). We also calculated the expected site frequency spectrum for 386 Argentine individuals genotyped on the Illumina exome chip, as described above. We used exome chip genotypes located in both filtered and unfiltered regions.

### Principal components analysis

We merged the Argentine GBS data with 1000 Genomes Project SNP data (CEU, YRI, and MXL populations), and with HGDP SNP data from sequenced Mayan individuals[28]. Of the segregating sites in the merged data set, 715,082 were present in each of the original data sets. We kept Argentine individuals that had  $> 25\%$  of these sites sequenced to  $\geq 7X$  (42/63 samples were kept). We then filtered out sites where  $< 90\%$  of all samples had called genotypes. We then applied the hard filters listed previously, and pruned SNPs for linkage disequilibrium ( $r^2 < 0.8$  in 50 bp windows with 5 bp step size) with PLINK[29], resulting in a final set of



45,630 SNPs. We performed principal components analysis on this set of SNPs with smartpca [30].

## Supporting Information

### S1 Text. Allele frequency estimation in GBS data sets by expectation-maximization.

(PDF)

**S1 Fig. Post-hoc re-quantification of Argentine GBS libraries.** **A.** The 10.38 kb bioanalyzer marker is used as an internal standard for DNA quantification, but if the sample to be quantified is overloaded or bleeds into the 10kb region of the electropherogram, the bioanalyzer software may overestimate the concentration of the marker, as shown here. This leads to incorrect estimation of the sample concentration. **B.** We reanalyzed bioanalyzer data from the first batch of 24 Argentine samples we sequenced, and plotted the total number of reads from each sample vs the quantity of DNA added to the final library pool based on the recalculated DNA concentration.

(PDF)

**S2 Fig. GBS SNP filtering.** **A.** The target region was defined to be the union of simulated digest fragments between 400–700 bp (200–600 bp for the Argentine samples) that had  $\geq 3X$  mean coverage per sample and where  $\geq 10\%$  of mate pairs were mapped to the restriction sites at the end of the fragment. **B.** Bioinformatics flowchart. SNP were called in the target region with GATK. Variant quality score recalibration (VQSR) was performed. Sites passing the basic filters had: mapping quality  $\geq 57$ , SNP quality  $\geq 30$ , coverage  $\geq 8X$  in all samples (HapMap samples) or coverage  $\geq 8X$  in  $\geq 40/63$  samples (Argentine samples), and position outside the 1000 Genomes Project callability mask. Sites failing the 1000 Genomes filter had  $> 10\%$  spanning reads mapped to known polymorphic restriction site (allele frequency  $> 0.01$ ). Sites failing the GBStools filter had: Non-cut allele frequency estimate  $> 0.05$ , or likelihood ratio  $> 2.71$  ( $p < 0.05$ ). Additional details on the filters are included in the methods section.

(PDF)

**S3 Fig. Coverage distributions for HapMap and Argentine GBS libraries.** **A.** Distribution of mean GBS coverage across eight HapMap samples for all sites in the genome, and for sites in the target region. **B.** Distribution of mean GBS coverage across the 63 Argentine samples that had  $\geq 30\%$  of reads mapped to restriction sites.

(PDF)

**S4 Fig. Effect of restriction site polymorphisms on genotyping accuracy and site frequency spectrum estimation in simulated GBS data.** **A.** Double-digest GBS genotype data ( $5 \times 10^5$  SNPs) were simulated for 100 diploid individuals under a neutral coalescent model with population mutation rates between  $1 \times 10^{-3}$  and  $2 \times 10^{-2}$ , and the genotype error rates plotted vs scaled mutation rate after removing sites with  $> 10\%$  missing genotypes. The error rates after removing sites with a GBStools likelihood ratio  $> 2.71$  are also shown for the same data with 40X mean coverage. **B.** Site frequency spectrum for restriction site polymorphisms for data simulated under a population mutation rate of  $1 \times 10^{-3}$ . Samples that carried two non-cut restriction site alleles were considered missing. **C.** The number of SNP genotyping errors is shown for each frequency class in B. **D.** The non-normalized SNP site frequency spectra for the same data as in A, represented as a subsample of size 50. **E.** The normalized site frequency spectra corresponding to those shown in D.

(PDF)

**S5 Fig. Dispersion of read coverage across samples at SNPs in HapMap GBS data set.** Target-region restriction sites were binned by mean coverage (bin width = 0.5), and dispersion index for coverage across samples (bin width = 0.1). The number of sites per bin is indicated by shade. Coverage was normalized at each site to account for variation in total read number per sample (methods). In estimating allele frequencies, GBStools used a fixed value for the dispersion index that was a linear function of the mean site coverage.

(PDF)

**S6 Fig. Quantile-quantile plots for restriction site polymorphism likelihood ratio statistic.**

**A.** The GBStools likelihood ratio statistic was calculated for SNPs in a simulated GBS data set that originated from a monomorphic restriction site, with either 8 or 100 samples, and with coverage of 10, 20, 30, 40, 50, 100, or 200X (methods). Each plot compares the quantiles of the likelihood ratio statistic to the quantiles of the expected null distribution, a one-half chi-squared distribution with one degree of freedom. **B.** Q-Q plots for sites in the simulated data where 4/16 or 4/200 chromosomes carried the non-cut restriction site allele. The power of the likelihood ratio test was calculated with a critical value of 2.71 ( $p < 0.05$ ).

(PDF)

**S7 Fig. Distributions of GBStools maximum likelihood parameter estimates for simulated GBS data with non-cut restriction site allele frequency = 0 (null model).** **A.** Estimates for the coverage parameter,  $\lambda$ , for the simulated GBS data set. **B.** Estimates for the non-cutter restriction site allele frequency parameter,  $\phi_3$ , for the simulated GBS data set.

(PDF)

**S8 Fig. Distributions of likelihood ratio statistic calculated from GBS read data at known polymorphic restriction sites.** The test statistic was calculated as described in S1 Appendix for 333,058 autosomal SNPs in the HapMap GBS data set that had  $< 25\%$  missing data. Each plot represents a group of SNPs that were sequenced to a different mean coverage, and within each group the test statistic is plotted versus the number of non-cut restriction site alleles present at the SNP. The blue lines represent the  $p = 0.05$  critical value from the theoretical null distribution, the one-half chi-squared distribution with one degree of freedom. The red lines represent the empirical  $p = 0.05$  critical value.

(PDF)

**S1 Table. Read mapping results for HapMap individuals.** Populations are annotated as YRI (Yoruban from Nigeria), MXL (Mexican American from Los Angeles), ASW (African-American from South West USA) and MKK (Maassai from Kenya). Genomes were sequenced with either Complete Genomics or ABI SOLiD technologies; read pairs are given per million (M), and coverage is given in fold-coverage. The target region is defined to be the union of simulated digest fragments between 400–700 bp that had  $\geq 3X$  mean coverage per sample and where  $\geq 10\%$  of mate pairs were mapped to restriction sites at the end of the fragment.

(PDF)

**S2 Table. Genotype concordance tables for HapMap and Argentine individuals with different combinations of filters.** **A-E.** HapMap samples (SNPs called with GATK UnifiedGenotyper). Sites are grouped by the Complete Genomics genotype call: homozygous reference (0/0), heterozygous (0/1), or homozygous non-reference (1/1). For each group, the proportion called 0/0, 0/1, or 1/1 by GBS is shown, followed by the total number of sites in the group. **F-G.** HapMap samples (SNPs called with GATK HaplotypeCaller). **H-K.** Argentine samples (SNPs called with GATK UnifiedGenotyper). Sites are grouped by the Illumina Exome Array

genotype call. A detailed description of the filters is provided in the methods section. (PDF)

**S3 Table. Area under curve (AUC) for response operator characteristic (ROC) curves.** The GBStools likelihood ratio test or Hardy-Weinberg equilibrium exact test p-values were used as classifiers of incorrect vs correct heterozygous genotype calls for simulated and empirical data, and sensitivity and specificity were calculated for various classifier thresholds (Fig 4A). There were  $2 \times 10^5$  sites in each simulated data set ( $\theta = 4N_e\mu = 1 \times 10^{-3}$ ), which included sites with and without restriction site variation. A 90% call rate filter was applied to the simulated data before calculating error rates, and "basic filters" (S2 Fig) were first applied to the HapMap and Argentine data. For reference, an uninformative (random) classifier has  $AUC = 0.5$  and a perfect classifier has  $AUC = 1.0$ . The total number of correctly called genotypes (non-error genotypes) and incorrectly called (error) genotypes are shown in the rightmost columns. (PDF)

**S4 Table. Read mapping results for Argentine individuals.** Read pairs are given per million (M), and coverage is given in fold-coverage, the final column indicates whether the samples were included (Y) or excluded (N) from the downstream analysis. The target region is defined to be the union of simulated digest fragments between 200–600 bp that had  $\geq 3X$  mean coverage per sample and where  $\geq 10\%$  of mate pairs were mapped to restriction sites at the end of the fragment. (PDF)

**S5 Table. Sequencing adapters.** Oligo sequence and barcode index for 65 sequencing adaptors used for library preparation. Adapters were made by annealing each of the index adapters #1–65 to the common adapter (methods). (PDF)

## Acknowledgments

The authors thank Suyash Shringarpure (Bustamante lab) for helpful suggestions, Brenna Henn and Jeffery Kidd for early access to the Mayan sequencing data, and Josefina MB Motti, Laura S Jurado-Medina, M Rita Santos, Virginia Ramallo, Marisol Schawb, Julieta Beltramo, and Mariela Cuello for help in collecting DNA samples, and the following groups from the University of Miami: Hussman Institute for Human Genomics, Center for Genome Technology, Genotyping Core, Biorepository Core.

## Author Contributions

Conceived and designed the experiments: TFC MCY MM OEC CDB EEK. Performed the experiments: TFC MCY MM AS RB OEC JLK CDB EEK. Analyzed the data: TFC MCY MM RB CDB EEK. Contributed reagents/materials/analysis tools: TFC MM GB CMB CDB EEK. Wrote the paper: TFC MCY MM AS CDB EEK.

## References

1. Altshuler D, Pollara VJ, Cowles CR, Van Etten WJ, Baldwin J, Linton L, et al. An SNP map of the human genome generated by reduced representation shotgun sequencing. *Nature*. 2000; 407: 513–6. PMID: [11029002](#)
2. Weber JN, Peterson BK, Hoekstra HE. Discrete genetic modules are responsible for complex burrow evolution in *Peromyscus* mice. *Nature*. 2013; 493: 402–5. doi: [10.1038/nature11816](#) PMID: [23325221](#)

3. Baird NA, Etter PD, Atwood TS, Currey MC, Shiver AL, Lewis Z a, et al. Rapid SNP discovery and genetic mapping using sequenced RAD markers. *PLoS One*. 2008; 3: e3376. doi: [10.1371/journal.pone.0003376](https://doi.org/10.1371/journal.pone.0003376) PMID: [18852878](https://pubmed.ncbi.nlm.nih.gov/18852878/)
4. Poland JA, Brown PJ, Sorrells ME, Jannink J-L. Development of High-Density Genetic Maps for Barley and Wheat Using a Novel Two-Enzyme Genotyping-by-Sequencing Approach. Yin T, editor. *PLoS One*. 2012; 7: e32253. doi: [10.1371/journal.pone.0032253](https://doi.org/10.1371/journal.pone.0032253) PMID: [22389690](https://pubmed.ncbi.nlm.nih.gov/22389690/)
5. Andersen EC, Gerke JP, Shapiro J a, Crissman JR, Ghosh R, Bloom JS, et al. Chromosome-scale selective sweeps shape *Caenorhabditis elegans* genomic diversity. *Nat Genet*. 2012; 44: 285–90. doi: [10.1038/ng.1050](https://doi.org/10.1038/ng.1050) PMID: [22286215](https://pubmed.ncbi.nlm.nih.gov/22286215/)
6. Hohenlohe PA, Bassham S, Etter PD, Stiffler N, Johnson E a, Cresko W a. Population genomics of parallel adaptation in threespine stickleback using sequenced RAD tags. *PLoS Genet*. 2010; 6: e1000862. doi: [10.1371/journal.pgen.1000862](https://doi.org/10.1371/journal.pgen.1000862) PMID: [20195501](https://pubmed.ncbi.nlm.nih.gov/20195501/)
7. Luca F, Hudson RR, Witonky DB, Di Rienzo A. A reduced representation approach to population genetic analyses and applications to human evolution. *Genome Res*. 2011; 1087–1098. doi: [10.1101/gr.119792.110](https://doi.org/10.1101/gr.119792.110) PMID: [21628451](https://pubmed.ncbi.nlm.nih.gov/21628451/)
8. Elshire RJ, Glaubitz JC, Sun Q, Poland J a, Kawamoto K, Buckler ES, et al. A Robust, Simple Genotyping-by-Sequencing (GBS) Approach for High Diversity Species. *PLoS One*. 2011; 6: e19379. doi: [10.1371/journal.pone.0019379](https://doi.org/10.1371/journal.pone.0019379) PMID: [21573248](https://pubmed.ncbi.nlm.nih.gov/21573248/)
9. Glaubitz JC, Casstevens TM, Lu F, Harriman J, Elshire RJ, Sun Q, et al. TASSEL-GBS: A High Capacity Genotyping by Sequencing Analysis Pipeline. *PLoS One*. 2014; 9: e90346. doi: [10.1371/journal.pone.0090346](https://doi.org/10.1371/journal.pone.0090346) PMID: [24587335](https://pubmed.ncbi.nlm.nih.gov/24587335/)
10. Arnold B, Corbett-Detig RB, Hartl D, Bomblies K. RADseq underestimates diversity and introduces genealogical biases due to nonrandom haplotype sampling. *Mol Ecol*. 2013; 22: 3179–90. doi: [10.1111/mec.12276](https://doi.org/10.1111/mec.12276) PMID: [23551379](https://pubmed.ncbi.nlm.nih.gov/23551379/)
11. Gautier M, Gharbi K, Cezard T, Foucaud J, Kerdelhué C, Pudlo P, et al. The effect of RAD allele dropout on the estimation of genetic variation within and between populations. *Mol Ecol*. 2012; 22: 3165–78. doi: [10.1111/mec.12089](https://doi.org/10.1111/mec.12089) PMID: [23110526](https://pubmed.ncbi.nlm.nih.gov/23110526/)
12. Davey JW, Cezard T, Fuentes-Utrilla P, Eland C, Gharbi K, Blaxter ML. Special features of RAD Sequencing data: implications for genotyping. *Mol Ecol*. 2013; 22: 3151–64. doi: [10.1111/mec.12084](https://doi.org/10.1111/mec.12084) PMID: [23110438](https://pubmed.ncbi.nlm.nih.gov/23110438/)
13. Fu X, Dou J, Mao J, Su H, Jiao W, Zhang L, et al. RADtyping: An Integrated Package for Accurate De Novo Codominant and Dominant RAD Genotyping in Mapping Populations. *PLoS One*. 2013; 8: e79960. doi: [10.1371/journal.pone.0079960](https://doi.org/10.1371/journal.pone.0079960) PMID: [24278224](https://pubmed.ncbi.nlm.nih.gov/24278224/)
14. Puritz JB, Matz M V, Toonen RJ, Weber JN, Bolnick DI, Bird CE. Comment : Demystifying the RAD fad. *Mol Ecol*. 2014; 1–18.
15. Peterson BK, Weber JN, Kay EH, Fisher HS, Hoekstra HE. Double digest RAD-seq protocol. *PLoS One*. 2012; 7: e37135. doi: [10.1371/journal.pone.0037135](https://doi.org/10.1371/journal.pone.0037135) PMID: [22675423](https://pubmed.ncbi.nlm.nih.gov/22675423/)
16. Drmanac R, Sparks AB, Callow MJ, Halpern AL, Burns NL, Kermani BG, et al. Human genome sequencing using unchained base reads on self-assembling DNA nanoarrays. *Science* (80-). 2010; 327: 78–81. doi: [10.1126/science.1181498](https://doi.org/10.1126/science.1181498) PMID: [19892942](https://pubmed.ncbi.nlm.nih.gov/19892942/)
17. Kidd JM, Gravel S, Byrnes J, Moreno-Estrada A, Musharoff S, Bryc K, et al. Population genetic inference from personal genome data: impact of ancestry and admixture on human genomic variation. *Am J Hum Genet*. 2012; 91: 660–71. doi: [10.1016/j.ajhg.2012.08.025](https://doi.org/10.1016/j.ajhg.2012.08.025) PMID: [23040495](https://pubmed.ncbi.nlm.nih.gov/23040495/)
18. DePristo MA, Banks E, Poplin R, Garimella K V, Maguire JR, Hartl C, et al. A framework for variation discovery and genotyping using next-generation DNA sequencing data. *Nat Genet*. 2011; 43: 491–8. doi: [10.1038/ng.806](https://doi.org/10.1038/ng.806) PMID: [21478889](https://pubmed.ncbi.nlm.nih.gov/21478889/)
19. Abecasis GR, Auton A, Brooks LD, DePristo M a, Durbin RM, Handsaker RE, et al. An integrated map of genetic variation from 1,092 human genomes. *Nature*. 2012; 491: 56–65. doi: [10.1038/nature11632](https://doi.org/10.1038/nature11632) PMID: [23128226](https://pubmed.ncbi.nlm.nih.gov/23128226/)
20. Hudson R. Generating samples under a Wright-Fisher neutral model of genetic variation. *Bioinformatics*. 2002; 18: 337–338. <http://bioinformatics.oxfordjournals.org/content/18/2/337.short> PMID: [11847089](https://pubmed.ncbi.nlm.nih.gov/11847089/)
21. Keinan A, Clark AG. Recent Explosive Human Population Growth Has Resulted in an Excess of Rare Genetic Variants. *Science* (80-). 2012; 336: 740–743. doi: [10.1126/science.1217283](https://doi.org/10.1126/science.1217283) PMID: [22582263](https://pubmed.ncbi.nlm.nih.gov/22582263/)
22. Catchen J, Hohenlohe PA, Bassham S, Amores A, Cresko WA. Stacks: an analysis tool set for population genomics. *Mol Ecol*. 2013; 22: 3124–3140. doi: [10.1111/mec.12354](https://doi.org/10.1111/mec.12354) PMID: [23701397](https://pubmed.ncbi.nlm.nih.gov/23701397/)
23. Li H, Durbin R. Fast and accurate short read alignment with Burrows-Wheeler transform. *Bioinformatics*. 2009; 25: 1754–60. doi: [10.1093/bioinformatics/btp324](https://doi.org/10.1093/bioinformatics/btp324) PMID: [19451168](https://pubmed.ncbi.nlm.nih.gov/19451168/)

24. Danecek P, Auton A, Abecasis G, Albers C a, Banks E, DePristo M a, et al. The variant call format and VCFtools. *Bioinformatics*. 2011; 27: 2156–8. doi: [10.1093/bioinformatics/btr330](https://doi.org/10.1093/bioinformatics/btr330) PMID: [21653522](https://pubmed.ncbi.nlm.nih.gov/21653522/)
25. Chernoff H. On the Distribution of the Likelihood Ratio Statistic. *Ann Math Stat*. 1954; 25: 573–578.
26. Marth G, Czabarka E, Murvai J, Sherry S. The allele frequency spectrum in genome-wide human variation data reveals signals of differential demographic history in three large world populations. *Genetics*. 2004; 372: 351–372. <http://www.genetics.org/content/166/1/351.short>
27. Nielsen R, Hubisz MJ, Clark AG. Reconstituting the frequency spectrum of ascertained single-nucleotide polymorphism data. *Genetics*. 2004; 168: 2373–82. PMID: [15371362](https://pubmed.ncbi.nlm.nih.gov/15371362/)
28. Raghavan M, Steinrücken M, Harris K. Genomic evidence for the Pleistocene and recent population history of Native Americans. *Science* (80-). 2015; 1–20. <http://www.sciencemag.org/content/early/2015/07/20/science.aab3884.short>
29. Purcell S, Neale B, Todd-Brown K, Thomas L, Ferreira M a R, Bender D, et al. PLINK: a tool set for whole-genome association and population-based linkage analyses. *Am J Hum Genet*. 2007; 81: 559–75. PMID: [17701901](https://pubmed.ncbi.nlm.nih.gov/17701901/)
30. Patterson N, Price AL, Reich D. Population structure and eigenanalysis. *PLoS Genet*. 2006; 2: e190. PMID: [17194218](https://pubmed.ncbi.nlm.nih.gov/17194218/)